# Rapid Food Particle Temperature Mapping During Ohmic Heating Using FLASH MRI

R. Ruan, P. Chen, K. Chang, H.-J. Kim, and I.A. Taub

**ABSTRACT**

**A fast low angle shoot (FLASH) pulse sequence in combination with a multi-inversion procedure was used to rapidly acquire spin-lattice relaxation data for food particles undergoing ohmic heating. The relaxation data acquired by magnetic resonance imaging (MRI) were analyzed using a two-component exponential model to extract both short and long spin-lattice relaxation time, $T_1$. The longer $T_1$ showed a better linear relationship with temperature than the shorter $T_1$ and, therefore, was used to produce more reliable temperature maps. The MRI temperature maps constructed for ohmically heated food particulates showed an entirely different heating pattern than would be found for similar but conventionally heated particulates and indicated that the temperature inside the particulate could be higher than near the surface of the particulate.**

**Key Words: MRI, ohmic heating, temperature mapping**

## INTRODUCTION

OHMIC HEATING IS PARTICULARLY WELL-suited for processing foods that contain particulates suspended in a carrier medium. Unlike conventional heating, which relies on heat transfer from the carrier medium to the particles, ohmic heating causes large food particles to heat at rates comparable to the surrounding liquid (Kim et al., 1995). Kim et al. (1996) demonstrated, using an industrial ohmic heating system and chemical and microbiological measurements, that the center of particulate foods received higher lethal treatment than the surface under typical conditions. However, ohmically heated products are not available in the U.S. market. A major concern has been whether the particles are adequately heated during ohmic heating to ensure sterility. Information on real-time temperature distribution in the carrier liquid medium and in the food particles is needed to obtain Food and Drug Administration approval of this advantageous thermal processing technology.

Mapping temperature or related indices in food materials undergoing processing is difficult and complex. Kim et al. (1995) used intrinsic chemical markers in conjunction with direct microbiological measurements for such temperature mapping. Sastry and Li (1996) reported a method that used temperature-sensitive liquid crystal sheets. Those methods provide information useful for process verification but are invasive. In addition, their results were obtained by post-processing analyses from limited regions within the collected particulates. Magnetic resonance imaging (MRI) can in principle provide effective, noninvasive temperature mapping for use in food science and technology (Schrader et al., 1992; Hill, 1995). However, there are problems with the use of MRI mapping techniques for monitoring temperature distribution in foods that are undergoing processing. Problems with long data acquisition time and effect of heating-induced structural changes on MRI parameters need to be better understood and overcome. Consequently, it is important to develop techniques that have the capability of fast tracking the changes in temperature that occur during a rapid heating process. It is also important to understand which MRI parameters best reflect thermal conditions of the materials and can be extracted from other MRI information.

The objective of this study was to develop a fast and reliable MRI technique for mapping temperatures in ohmically heated particulate foods.

*Authors Ruan, Chen, and Chang are affiliated with the Dept. of Biosystems and Agricultural Engineering and Dept. of Food Science and Nutrition, Univ. of Minnesota, St. Paul, MN 55108. Author Kim is with the Dept. of Chemistry, College of Natural Sciences, Seoul National Univ., Seoul 151-742, Korea. Author Taub is with the Office of Technical Director, U.S. Army Natick Soldier Center, Natick, MA 01760-5018. Address inquiries to Dr. Roger Ruan* [redacted]

## MATERIALS & METHODS

### Ohmic heating of particulate foods

Particulates studied were potato, carrot, and beef. They were cut into about 2.5 $cm^3$ cubes. The carrier medium was made up of 50 g/kg starch and 1 g/kg NaC1. An experimental ohmic heating device was constructed of glass, including a 38-mm dia and 318-mm long glass tube with a rubber stopper at each end (Fig. 1). A 30-mm dia stainless still electrode was fixed to each of the stoppers and connected to a transducer corresponding to a 50 Hz AC power supply. A hole was made in one of the stoppers to allow release of pressure built up within the tube during heating. Two fiber optic temperature sensors could be inserted into the tube through this hole, one near the end of the tube and the other in the center. A constant 140 volts was applied.

### MRI Instrumentation

A custom-made volume birdcage radio frequency (RF) coil that fitted the configuration of the heating tube was used as both the RF transmitter and MR signal receiver. Substantial adjustments were made to carefully shim the magnetic field to achieve narrow linewidth of the MR spectrum of the sample in the heating tube. The coil proved to be the key to the successful application of MRI in this study. The ohmic heating tube was placed in the center of the coil (Fig. 1). The metallic electrodes at both ends of the heating tube were kept out of the effective RF field to avoid interference.

A 4.7 Telsa SISCO imaging spectrometer (Varian, Palo Alto, Calif.) with a 330-mm dia bore, superconducting magnet was used. The fast low angle shoot (FLASH) pulse sequence in combination with an inversion procedure was used to acquire data needed to construct $T_1$ images.

### Data acquisition during heating

Heating at a constant voltage was controlled by the transducer. It was interrupted during data acquisition to avoid interfering with the electric field. Data were collected at heating times of 1, 5, 8, 11, 13.25, 13.5, 13.75 (ohmic heating was completely stopped at this point), 28.75 (holding), and 38.75 (holding) min (Fig. 2). The last two data points were collected to observe heat

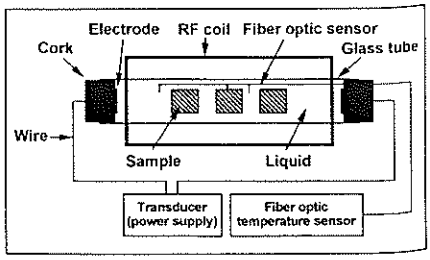


**Fig. 1—Schematic of ohmic heating device incorporated into the MRI instrument.**



© 1999 Institute of Food Technologists

transfer between the particulate and the suspending fluid after terminating the energy input. The temperature of the liquid was also recorded during and after electrical energy input.

The time for acquisition of a single image was greatly reduced by using the inversion-recovery FLASH sequence. This pulse sequence involved multiple inversion-recovery pulses, that is, the signal was always reverted to the negative maximum and then allowed to recover for some time prior to data acquisition. This process was repeated many times with stepwise increasing recovery time, until the magnetization returned to its positive maximum. Thus, an exponential curve of recovery time vs signal intensity was produced. The total data acquisition time, ranging from several seconds to tens of seconds, would depend on the number and length ($T_i$) of inversion-recovery cycles and would amount to = $\Sigma T_i$. Seven inversion-recovery cycles, with an increasing step of 0.3 s and a delay time of 0.8 s, were used in data acquisition. Therefore, the total time for acquiring 7 signal intensity images for construction of a single $T_1$ image (128 × 128 pixels) was about 14 s, compared to several minutes for spin-echo sequence, a commonly used pulse sequence for $T_1$ mapping.

### $T_1$ fitting and mapping

Each data acquisition procedure resulted in 7 signal intensity images with identical geometric dimensions but different recovery times. Each pixel in each of the 7 images had a signal intensity value. The relationship between the recovery time and signal intensity can be described by Eq (1) or (2), which are one-component and two-component models, respectively:

$$S = M_0(1 - 2e^{-\frac{T_i}{T_1}}) \quad (1)$$

$$S = M_1(1 - 2e^{-\frac{T_i}{T_{1S}}}) + M_2(1 - 2e^{-\frac{T_i}{T_{1L}}}) \quad (2)$$

where $T_i$ is the inversion time, $T_{1S}$ and $T_{1L}$ are the short and long $T_1$, respectively.

These mathematical relationships can be applied to the same spot (pixel) of the 7 images to calculate a $T_1$ value, and, therefore, the $T_1$ values calculated from the 7 images form a new $T_1$ image. It has been generally assumed in most reports that $T_1$ is a linear function of temperature.

However, various experiments suggest that a change in structure and moisture causes noticeable differences in $T_1$, and, thus, an appreciable error would be obtained if temperature were calculated from undescriminated $T_1$ values of Eq (1). The error would be greater when foods undergo heat-induced alterations in structure and moisture during heating. The two-component model corresponding to Eq (2) involves 2 $T_1$ values, each representing a fraction of the protons in the sample. The shorter $T_1$ is the more strongly structure-dependent term, therefore the longer $T_1$ would be a more reliable indicator of temperature in foods.

Examples of the fitting (Fig. 3) showed that the one-component model fitted the data very poorly, while the two-component model fitted the data perfectly.

### Calibration between $T_1$ and temperature

Calibration was done by measuring the signal intensity of a spot in the MR image, where the temperature was measured using the fiber optic temperature sensors. This procedure was repeated for several spots and at different temperatures. The relationship between $T_1$ and temperature (θ) was determined using a linear function as follows

$$T_1 = \alpha + b\theta \quad (3)$$

where $a$ and $b$ are constants related to the nature of the material. This calibration was carried out for each material.

Data indicated that $T_{1S}$ and temperature did not conform to a linear relationship (Fig. 4), indicating that $T_{1S}$ might be influenced by secondary factors that varied with temperature. In contrast, $T_{1L}$ was shown to be linearly related to temperature (Fig. 5), confirming our previous assumption that $T_{1L}$ is less influenced by structural changes.

To translate the $T_1$ data into temperature for a particle, the relationship described by the above equation was applied within the boundary of the particle. This translation procedure was automated using a computer program that discerns the true signals from background noise and then applies the temperature fit to the true signals only. The temperature data files were processed on a Macintosh computer using the public domain NIH Image 1.57 program (developed at the U.S. National Institutes of Health and available on the Internet at http://rsb.info.nih.gov/nih-image/) to produce two-dimensional images and surface plots.

## RESULTS & DISCUSSION

WHEN ENERGIZED TO 140 VOLTS, THE EXperimental ohmic heating device produced an initial heating rate of about 4 °C/min in the liquid phase, depending upon the liquid composition. Within the range of NaCl concentration tested (0 to 0.5 g·kg$^{-1}$), a higher concentration in the liquid phase produced a faster heating rate. We also found that heating rates increased gradually with heating time or increasing temperatures (Fig. 2). It took about 13 min for the liquid to reach 95 °C.

The MRI images (Fig. 6) and the surface plots (Fig. 7) constructed from these images show that the temperature in the particulates and the corresponding rate of heating the particulates increased with heating time. The increased heating rate was consistent with the rise in electrical conductivity of the particulates with temperature. Wang and Sastry (1995) reported a higher electrical conduc-

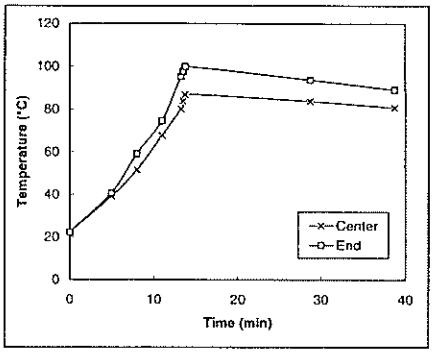


**Fig. 2—Temperature of liquid as a function of time. Heating was terminated at 13.75 min.**

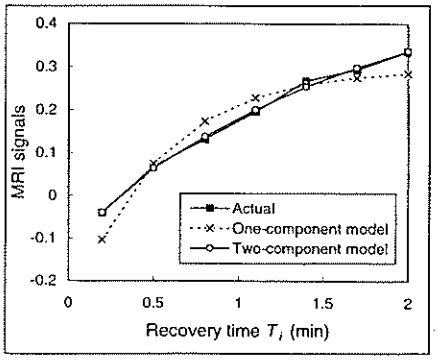


**Fig. 3—Fitting of one-component and two-component models. $T_1$ data.**

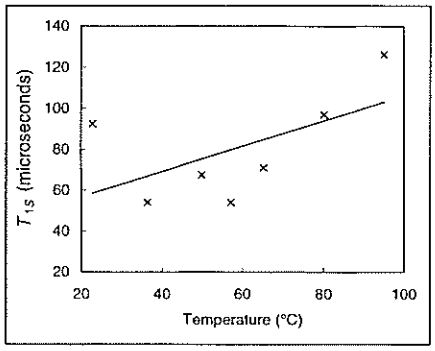


**Fig. 4—Relationship between the shorter $T_1$ ($T_{1S}$) and temperature (in beef).**

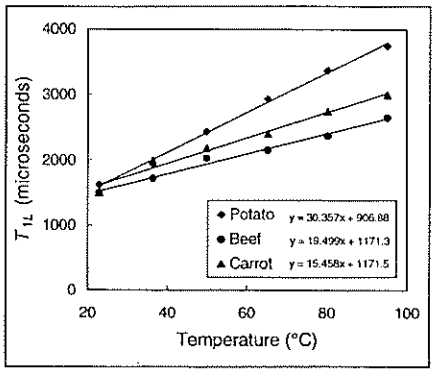


**Fig. 5—Relationship between the longer $T_1$ ($T_{1L}$) and temperature in potato, beef and carrot.**

tivity for ohmically heated materials compared to unheated raw materials. An increase in heating rate with time was also observed in the liquid phase (Fig. 2), reflecting the increase in electrical conductivity with temperature.

These images indicate differences in temperature among different particulates in the same carrier fluids. Beef appeared to heat faster than other foods. The differences in heating rate among different materials could be due to differences in electrical conductivity (Kim et al., 1996) and/or nonuniformity in the electric field. When two temperature probes were placed in different locations within the heating tube, the observed temperature variation was considerable (Fig. 2).

The MR images also show that the temperatures in the center regions of a particulate were higher than in the outer regions, indicating that the particulate heated intensively and transferred heat to the colder carrier liquid. Variation in temperature was observed within a particle, probably due to spatial variation in electrical conductivity. Two additional images (Fig. 6 and 7), taken 28.75 and 38.75 min after heating was terminated, show that the heat redistributed within the particulates. These results indicate that, in modeling the ohmic heating process, the generation of heat and associated distribution of temperatures during the heating stage and the redistribution of temperatures during the holding stage all need to be taken into consideration.

The MRI temperature mapping techniques could be used to validate the adequacy of mathematical models for ohmic heating of particulates in a liquid carrier medium. This validation is essential for process design and control. If both the carrier medium and the food particles need to be treated to achieve the same degree of bacterial destruction (i.e., lethality), then a procedure should be designed to ensure that both media have similar electrical conductivity, or more precisely, heating rate. Alternatively, the procedure could be designed so the particulates heat faster than the carrier medium. Both could be done by treating the solid materials with salt solution prior to heating and changing the composition of carrier fluids. The effect of such treatments on the temperature distribution in the materials could be evaluated by the MRI techniques so that adjustment in treatment conditions could be made.

The inversion-recovery FLASH technique is very suitable for use with high moisture content materials. For low moisture content materials, a low signal-to-noise ratio may result due to the use of low angle shoot sequence, which generates weaker signals than ordinary pulse sequence, and may, thus, compromise the quality of images.

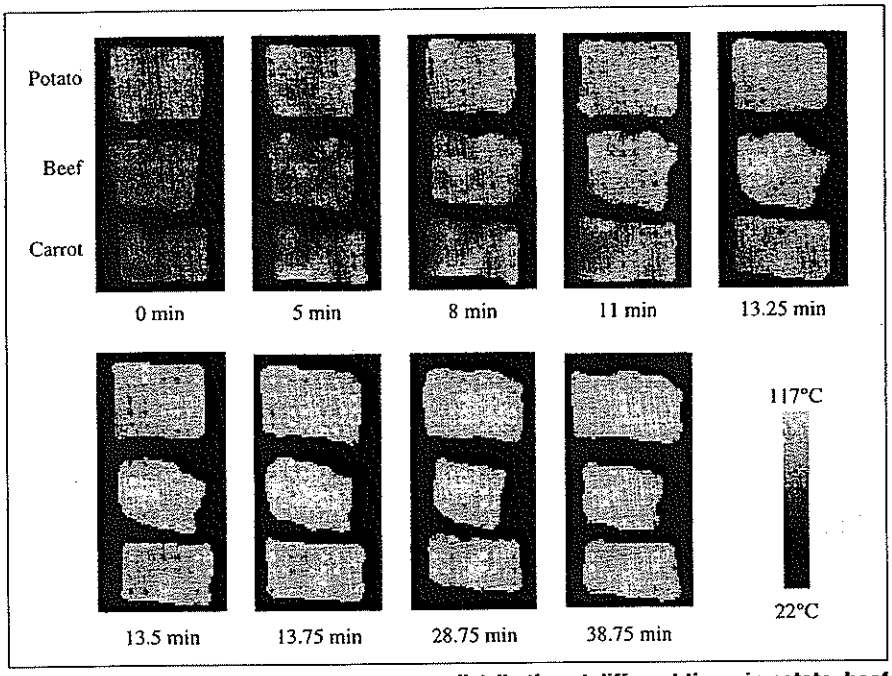


**Fig. 6—2-D MR images showing temperature distribution at different times in potato, beef and carrot cubes undergoing ohmic heating. Heating was terminated after 13.75 min.**

## REFERENCES

Hill, B. 1995. Food processing: an MRI perspective. Trends Food Sci. Technol. 6: 111-117.

Kim, H.J., Choi, Y.M., Heskitt, B., Sastry, S.K., and Li, Q. 1995. Chemical and microbiologicalinvestigation of ohmic heating of particulate foods using a static ohmic heater. Presented at Annual Meeting of Inst. of Food Technologists, Anaheim, Calif., June 3-7.

Kim, H.J., Choi, Y.M., Yang, T.C.S., Taub, I.A., Tempest, P., Skudder, P., Tucker G., and Parrot, D.L. 1996. Validation of ohmic heating for quality enhancement of food products. Food Technol. 50 (5): 253-261.

Sastry, S.K. and Li, Q. 1996. Modeling the ohmic heating of foods. Food Technol. 50(5): 246-248.

Schrader, G.W., Litchfield, J.B., and Schmidt, S.J. 1992. Magnetic resonance imaging applications in the food industry. Food Technol. 46(12): 77-83.

Wang, W.C. and Sastry, S.K. 1995. Changes in electrical conductivity of selected vegetable stuffs during multithermal treatments. Presented at Annual Meeting of Inst. of Food Technologists, Anaheim, Calif., June 3-7.

Ms 5368 received 12/12/98; revised 6/25/99; accepted 7/9/99.

We thank the U.S. Army Natick Soldier Center for financial support.

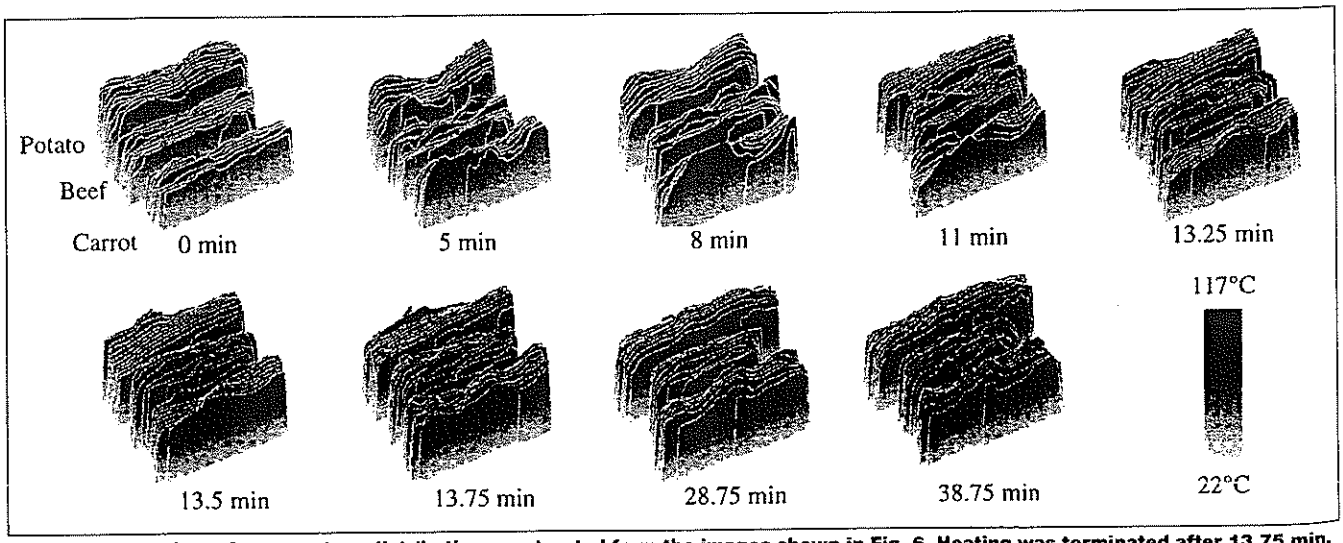


**Fig. 7—Surface plots of temperature distribution constructed from the images shown in Fig. 6. Heating was terminated after 13.75 min.**